New Journal of Physics
The open access journal for physics

Micro-rheological behaviour and nonlinear rheology of networks assembled from polysaccharides from the plant cell wall

R R R Vincent[1], B W Mansel[2,3], A Kramer[4], K Kroy[4] and M A K Williams[2,3,5,6]

[1] IBEC, C/Baldiri Reixac 10-12, E-08028 Barcelona, Spain
[2] Institute of Fundamental Sciences, Massey University, Palmerston North, New Zealand
[3] MacDiarmid Institute for Advanced Materials and Nanotechnology, New Zealand
[4] Institute for Theoretical Physics, Universität Leipzig, Brüderstraße 16, 04103 Leipzig, Germany
[5] Riddet Institute, Massey University, Palmerston North, New Zealand
E-mail: m.williams@massey.ac.nz

New Journal of Physics **15** (2013) 035002 (21pp)
Received 21 October 2012
Published 1 March 2013
Online at http://www.njp.org/
doi:10.1088/1367-2630/15/3/035002

Abstract. The same fundamental questions that have driven enquiry into cytoskeletal mechanics can be asked of the considerably less-studied, yet arguably just as important, biopolymer matrix in the plant cell wall. In this case, it is well-known that polysaccharides, rather than filamentous and tubular protein assemblies, play a major role in satisfying the mechanical requirements of a successful cell wall, but developing a clear structure–function understanding has been exacerbated by the familiar issue of biological complexity. Herein, in the spirit of the mesoscopic approaches that have proved so illuminating in the study of cytoskeletal networks, the linear microrheological and strain-stiffening responses of biopolymeric networks reconstituted from pectin, a crucial cell wall polysaccharide, are examined. These are found to be well-captured by the glassy worm-like chain (GWLC) model of self-assembled semi-flexible filaments. Strikingly, the nonlinear mechanical response of these pectin networks is found

[6] Author to whom any correspondence should be addressed.

to be much more sensitive to temperature changes than their linear response, a property that is also observed in F-actin networks, and is well reproduced by the GWLC model. Additionally, microrheological measurements suggest that over long timescales (>10 s) internal stresses continue to redistribute facilitating low frequency motions of tracer particles.

Contents

1. Introduction

1.1. Mesoscopic models

Much progress has been made recently in the study of the mechanical properties of solutions and networks of semi-flexible protein filaments, driven largely by the desire to understand the functionality of the cytoskeleton [1–6]. Indeed, the results gleaned from the study of such biologically relevant structures as F-actin have been exploited by soft-matter physicists interested in modelling the behaviour of all manner of semi-flexible filaments [7–10]. In particular the worm-like chain (WLC) model of polymer physics [11, 12] has found considerable utility in describing the dynamics and the force-extension behaviour both of single biopolymer chains, and of higher-order semi-flexible assemblies such as multimeric filaments, ribbons, tubes and worm-like micelles. Generally speaking the malleable mechanics and slow dynamics characteristic of soft and biological matter arises from the thermo-reversible assembly of low-dimensional manifolds into (transient) meso-structures.

In order to understand the time and length-scale dependent rheological properties of such systems, the central task is to understand how the interactions interfere with the dynamics of the individual constituents. Inspired by the underlying similarity of constraint release in these systems and the thermally-activated jumping between local traps in soft glasses [13, 14], the glassy worm-like chain (GWLC) model [15–17] addresses this problem by exponentially stretching the relaxation spectrum for single-chain motions involving wavelengths beyond

a characteristic backbone length, Λ. While the exponential form of the stretching is not microscopically derived, the model builds on the known mesostructure of the polymer network, and introduces a single 'stickiness' parameter that intuitively corresponds to the characteristic depth of the potential well that a cross-linked chain section must escape in order to dissociate. Despite its simplicity, the model has been successfully used to parameterize the frequency-dependent linear rheology of such systems, their nonlinear strain-stiffening behaviour, and additionally, by considering the stress dependence of the number of cross-links, their eventual softening [18].

The GWLC theory has not however been previously applied to the analysis of polysaccharide systems, despite the fact that they too play a significant role in controlling the mechanical properties of tissues, ranging from mammalian connective tissues to the ubiquitous plant cell wall. Herein, pectin gels have been studied to test the utility of existing models in describing the rheological properties of networks of this important class of carbohydrate biopolymers. Specifically the acid-gel system was selected where the 'stickiness' of the interaction between network strands originates from hydrogen bonding between extended patches on different chains. Microrheological studies were undertaken using (i) diffusing wave spectroscopy (DWS), which maximizes the accessible frequency range and (ii) multiple-particle tracking (MPT), which allows the homogeneity of the system to be probed. In addition measurements of the stress–strain behaviour following the application of varying pre-stresses were carried out. Results are discussed within the framework of models of semi-flexible networks and slow, glassy network relaxation.

2. Materials and methods

2.1. Materials

2.2. Pectin

2.2.1. Pectin structure. Pectin is a complex polysaccharide of the plant cell wall that is thought to be a crucial player in the control of its mechanical functionality [19]. Indeed, a recent reappraisal of cell wall mechanics and growth control suggests not only that pectin is crucial in this regard in Charophycean algae, the closest relatives of land plants, but that a primitive pectin-based control mechanism may still be functional in terrestrial plants. In this context, it has been proposed to be operating in parallel to more recently evolved and more widely-studied mechanisms involving cellulose, xyloglucans and expansins [20]. While the detailed structure of pectin is still a matter of debate to some extent [21] the preponderance of homogalacturonan (HG) regions within the macromolecular chains is well established. These regions consist of the order of 100 sugar residues connected together by axial 1–4 linkages and are essentially co-polymers of two types of sugar ring: galacturonic acid and its methylesterified counterpart (figure 1). Depending upon the pH-controlled protonation state of the bare galacturonic acid group, and the enzymatically controlled pattern of the uncharged but hydrophobic methylester substituents this yields chain sections that have varying local charge densities and differing propensities to associate through polyelectrolytic, specific ion, hydrophobic or hydrogen bonding effects. These HG regions are primarily responsible for the associations between chains, and from a physical point of view, offer the exciting possibility of tuning the interaction potentials by various mechanisms.

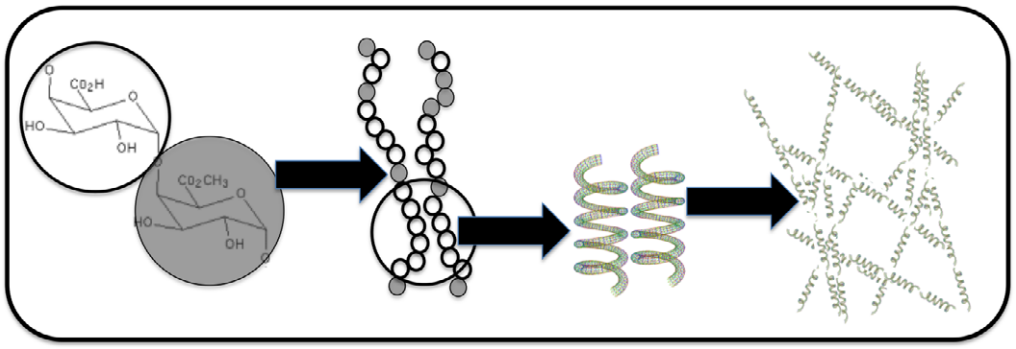

Figure 1. Molecular to mesoscopic: a schematic diagram showing the molecular structure of the pectin used herein, its proposed assembly mechanism in conditions of low pH, and larger-scale formation of a network.

2.2.2. Pectin assembly. *In vivo*, one mechanism employed in network building is the cross-linking of the chains by employing calcium ions to bridge runs of contiguous charged sugar residues on HG components of different polymeric backbones. The importance of the pectin methylesterase (PME) enzymes in controlling the amount and distribution of uncharged methylester groups is highlighted by the fact that around ten consecutive charged residues on each HG are required to form stable calcium-mediated junctions at room temperature [22–25]. Such ionotropic pectin gels have been considered as a simple model of the middle lamellar of primary plant cell walls and a reasonable description of the pollen tube [26] and indeed recent work has focused on utilizing plant-cell-wall enzymes to release the ion-binding galacturonic-acid-sequences in an attempt to model biomimetic processes of network formation [27–30]. The study of more traditional calcium-set gels where the ions are either introduced into hot pectin solutions that are then cooled or are released slowly from the dissolution of sparingly soluble salts under ambient conditions has a long history [19], owing primarily to the industrial relevance of such systems in food processing.

By contrast, it was only relatively recently that it was demonstrated that highly concentrated solutions ($\sim 10\,c^*$) of pectins containing limited amounts of the methylesterified version of the sugar rings (low degree of methylesterification (DM)) could also form networks in the absence of ions at low pH [31]. Subsequently it was shown that pectic polymers displaying more extreme contiguous intramolecular arrangements of the unmethylesterified galacturonic acid groups could in fact form acid-induced networks at much lower polymer concentrations, similar to those familiar in the more traditional calcium-mediated systems [32]. There is good experimental evidence from chiroptical methods, calorimetry, potentiometry and NMR to suggest that, as the pH is lowered in these systems and the charged residues are progressively protonated, the preferred polysaccharide conformation about which the solution-state structure fluctuates changes from being a two-fold extended helix to a more compact three-fold structure [33–35]. In its turn this conformational change favours the lateral aggregation of chains between anti-parallel three-fold helical stretches via hydrogen bonding [36, 37]. This hydrogen bonding, that is ultimately responsible for the association of the chains into a stress-bearing meso-scale network, involves interactions between protonated or charged carboxyl moieties and thus clarifies the detrimental effect of methylesterification in these systems. The presence of methylester groups reduces the pH sensitivity of the intramolecular conformational

changes and hinders the zipping together of intermolecular junction zones that require concerted runs of hydrogen bonds in order to form relatively thermally stable connections. The propensity of the polymers to form such zipped junction-zones is similarly maximized in samples in which the methylester content has been reduced using plant derived PME enzymes that are known to produce extreme contiguous sequences of bare galacturonic acid residues. While the relevance of these acid-gels, assembled primarily from hydrogen-bonded associations, is unclear at present for the native plant cell wall compared to their calcium-assembled cousins, these systems are considerably more thermoreversible than their ionotropic counterparts and as such are convenient model systems for experiments on semi-flexible networks (figure 1).

2.2.3. Pectin. Pectin (Mw 30–100 kDa), extracted from apple pomace, was purchased from Fluka Biochemika (Sigma Aldrich, Switzerland) as a starting material. The sample average DM and the degree of blockiness [32] of this sample, and that produced by modification as described below, were determined using capillary zone electrophoresis as previously described [39, 40].

2.2.4. Pectinmethylesterase. Pectinmethylesterase (EC 3.1.1.11) was purchased from Sigma Aldrich (P5400) in order to remove methylester groups from the starting pectin in a contiguous manner. Stock solutions of the enzyme were prepared by dissolving 0.01 g of dried PME in 20 ml in Milli-Q water, and were stored at −20 °C in Eppendorf tubes. Aliquots were thawed prior to conducting experiments and used immediately.

2.2.5. Polygalacturonase. Polygalacturonase (EC 3.2.1.15) was used to digest the polymeric substrates in order to verify a contiguous intramolecular distribution of the unmethylesterified (acidic) groups. The enzyme was kindly provided by Jacques Benen from the University of Wageningen. It is a pure endo-PG II isoform from *Aspergillus niger* and has an absolute requirement for the sugar residues in the active site to be unesterified in order for the chain to be severed, which yields the degradation pattern methylester-sequence dependent. A 1 ml solution of substrate at a concentration of 0.5% w/w and pH 4.2 (acetate buffer 50 mM) was incubated with 20 μl of enzyme solution (0.094 mg ml^{-1} protein). At the end of the reaction, the enzyme was denatured at 90 °C for 3 min and the oligosaccharides liberated by the digestion were quantified using capillary electrophoresis as previously described [41–43].

2.2.6. Polystyrene. Polystyrene tracer particles, either with a diameter of 505 nm or fluorescently-labelled with a diameter of 546 nm were purchased from Polyscience Inc. (Warrington, PA) (2.62% w/v stock solutions) for use as microrheological probes.

2.2.7. Pectin fine structure engineering. Pectin solutions of 1% w/w were made by dissolving pectin powder in a 50 mM 4-(2-hydroxyethyl)-1 piperazineethanesulfonic acid (HEPES) buffer, adjusted to pH 7.5 with NaOH. 0.5 ml of enzyme solution was then mixed into 30 ml of solution, and the solutions were left at 20 °C for a chosen time, depending on the final DM decrease required and on the rate of the de-methylesterification processes. Assuming the enzyme reaction followed a simple Michaelis–Menton law and were in the linear section of the product production curve (which was monitored independently using NMR to follow the liberation of methanol [44]), preliminary experiments were used to determine the rate of DM decrease as 4% per hour for the plant PME de-methylesterification used. Thus, the PME action could be

stopped after a pre-requisite time in order to achieve a desired final DM. This was carried out by decreasing the pH and subsequently heating the solution to 80 °C for 5 min to denature the enzyme. The modified polymers were extracted by dialysing twice against Milli-Q water. The dialysed solutions were freeze-dried and the engineered polymers recovered and stored dry. The recovered pectin samples had their fine structures analysed by capillary electrophoresis, which characterized the sample-average DM of the pectin, and provided evidence of the distribution of the acidic residues by analysing the endo-PG II-digest products. The result of this measurement was crucial as it confirmed our ability to prepare a polymer with the propensity to form long contiguous runs of hydrogen bonded sugar rings, unhindered by the presence of methylester substituents.

2.2.8. Acid induced gels. The acid-induced gels studied herein were obtained by gradually decreasing the pH of solutions of a pectin of DM $(42 \pm 4)\%$, (designated DM42) that had been obtained by PME modification of a more highly methylesterifed starting pectin as described above. This polymer was confirmed (by the dominance of unmethylesterified oligomers present in its endo-PG II digest pattern) to have a highly blockwise distribution of its unmethylesterified, bare galacturonic residues. The acidification of the polymer solution was performed slowly over a few hours, initiated by the addition of glucono delta-lactone (GDL) to the polymer solutions, which slowly hydrolyses releasing protons (figure 2(a), inset). While low DM pectins are known to be capable of forming gelling systems under simple acidification [30], polymers with blocky fine structures as engineered herein have been found to have a greater propensity to assemble under these conditions than those with the same DM but a random distribution thereof [32]. Indeed, at 1% polymer concentration preliminary experiments (data not shown) on various low-DM pectin solutions found that upon acidification (i) a DM 35% pectin with a random distribution of its acidic residues showed no discernable change in its materials properties, (ii) a DM of 37% sample with a medium blockiness simply viscosified slightly and (iii) the more blockwise 42% sample studied in depth here formed a respectable gel network. This indicates that long contiguous blocks of acidic residues (longer than those required to chelate calcium into a stable cross-link for example) are indeed necessary to form stable junction zones under these conditions, consistent with the idea of weak but concerted hydrogen bonded junctions being formed when the pH is decreased.

To form the gels the required amount of a pectin stock solution of 2% w/w adjusted to pH 7, bead solution (for DWS experiments and MPT), Milli-Q water and GDL were mixed in order to achieve a polymer concentration of 1% w/w and an initial GDL concentration of 8% w/w. The solution was quickly loaded into the appropriate sample cell and left to set for 24 h. The final pH of the gels studied was around 2, below the approximate pK_a of the galacturonic acid groups (3.5–4.5), and well within in the acid-gel forming domain found previously [31].

2.3. Microrheology

The aim of microrheology is to extract the rheological properties of soft materials from the motion of probe particles immersed in the material [45–47]. It is a non-destructive technique and recovers the linear response of the material. The essential quantity that passive microrheology experiments set out to measure is the mean square displacement (MSD) of tracer particles, which can be acquired to high frequencies using DWS or in a spatially resolved fashion with MPT.

2.3.1. Diffusing wave spectroscopy. The DWS apparatus used in this study is based on a system that has been fully described previously [48]. The samples were contained in polystyrene cells of width 10 mm, height 50 mm and path length L of 4 mm, and were illuminated with a 35 mW He–Ne Melles-Griot laser operating at 633 nm. The laser beam was expanded to approximately 8 mm on the surface of the cell. The transmitted scattered light was detected using a graded-index (GRIN) lens and a single-mode optical fibre (P1-3224-PC-5, Thorlabs Inc., Germany), which was typically split by a fibre optic beam splitter and sent to two Hamamatsu HC120-08 PMT photomultiplier-tube modules. The correlation function was then calculated using a cross-correlation method in software on a standard personal computer. Using cross-correlation helped circumvent dead-time in the electronics as well as eliminating after-pulsing effects. Tests were run for between 10 and 100 min to minimize noise. The temperature was controlled using a TLC 50 temperature-controlled cuvette holder purchased from Quantum Northwest (www.qnw.com), which uses a thermoelectric device. For heat removal, a small flow of water passes through a heat exchanger and a calibrated TC 125 temperature controller was used with a thermistor to control the temperature to within 0.1 °C. For an expanded beam mode, the field autocorrelation function is obtained from the measured intensity autocorrelation function using the Siegert equation. In the transmission geometry, the field correlation function has been given by Weitz and Pine [49] and once the light mean free path is determined, the MSD can be obtained from the experimental correlation functions by inverting them with a zero-crossing routine.

2.3.2. Multiple-particle tracking. An inverted microscope (Nikon Eclipse TE2000-U) on an air damped table (photon control) equipped with a mercury lamp (X-cite Series 120PC EXFO) and a 60x 1.2 NA (Nikon, Plan Apo VC 60x WI) water immersion objective lens was used for MPT experiments. Samples were gelled in welled microscope slides and sealed with a cover slip. A CCD camera (Foculus FO124SC) was used to record image series taken for up to 100 s; at 43 frames per second. Typically around 40 individual particles were tracked in any one experiment. x–y coordinate data was extracted from the movies using a homebuilt program written using algorithms obtained from: http://physics.georgetown.edu/matlab/. In-house programs to calculate the MSD and Van Hove correlation function were used in combination with a program to de-drift the data obtained from: http://people.umass.edu/kilfoil/downloads.html.

2.4. Pre-stress experiments

A stress controlled ARG2 rheometer from TA Instruments (Delaware, USA) was used with a cone and plate geometry of 40 mm diameter and a cone angle of 4°. The linear complex modulus was determined by applying small amplitude strain oscillations (0.1%) at 1 Hz, and the normal force was also recorded at every time step. Pre-stress experiments were performed by superimposing small-amplitude stress-oscillations, $\mathrm{d}\sigma$, on top of a constant pre-stress σ_0 [50]. The differential stiffness was then computed for different pre-stresses according to

$$K = \frac{\mathrm{d}\sigma}{\mathrm{d}\gamma} \tag{1}$$

with $\mathrm{d}\gamma$ being the measured small-amplitude strain oscillation. The temperature was controlled using a Peltier system to within 0.1 °C.

2.5. Glassy worm-like chain model

2.5.1. Differential shear modulus. In the GWLC model, the microscopic susceptibility is given by

$$\alpha_f(\omega) = \frac{L^4}{k_B T \pi^4 l_p^2} \sum_{n=1}^{\infty} \frac{1}{(n^4 + n^2 f/f_L)(1 + i\,\omega\tilde{\tau}_n/2)}, \tag{2}$$

where L is the polymer length, l_p the persistence length, f an optional backbone tension, and $f_L = \kappa\pi^2/L^2$ the Euler buckling force of a rod with bending rigidity κ [12]. The mode relaxation time $\tilde{\tau}_n$ is given by

$$\tilde{\tau}_n = \begin{cases} \tau_n & (\lambda_n < \Lambda), \\ \tau_n \exp[\mathcal{E}(\lambda_n/\Lambda - 1)] & (\lambda_n \geqslant \Lambda), \end{cases} \tag{3}$$

where

$$\tau_n = \frac{\tau_L}{n^4 + n^2 f/f_L} \quad \text{with} \quad \tau_L = \frac{\zeta_\perp L^4}{\kappa\pi^4} \tag{4}$$

is the mode relaxation time of the WLC. For wavelengths $\lambda_n \equiv L/n$ longer than the typical contour length Λ between neighbouring bonds, the relaxation is stretched by an Arrhenius factor, where the stretching parameter $\mathcal{E}$ controls the slowing down of the dynamics, which is understood to be caused by the interactions of the test polymer with the surrounding polymer network.

The stretching parameter $\mathcal{E}$ is interpreted as the height of a characteristic barrier in units of $k_B T$. It may be either enhanced or lowered by external or internal stresses, which are therefore coupled into the Arrhenius factor in equation (3) as follows:

$$\mathcal{E} \to \mathcal{E} \pm f/f_T \quad \text{with} \quad f_T \equiv k_B T/\Delta, \tag{5}$$

where f_T represents the scale of the thermal equilibrium tension present in a force-free sample, and Δ the characteristic width of the free energy barrier. For the fits in the following, we invariably assume that the negative sign holds in equation (5). Within this scheme, the shear modulus of the prestressed sample is equivalent to the nonlinear differential shear modulus [38]:

$$K^*(\omega) = \frac{c}{15}\frac{\rho\Lambda}{\alpha_f(\omega)} - i\,\omega\eta, \tag{6}$$

where $\rho \equiv 3/\xi^2$ is the contour length concentration, ξ the mesh size, η the solvent viscosity and c a numerical fitting parameter that is needed to adapt the prediction derived for homogeneous semiflexible networks to our case, where the precise relation between the microstructural parameters and the meso-structure is *a priori* not known.

Experimental data can be fitted to the model by inserting the microscopic susceptibility $\alpha_f(\omega)$ from equation (2) into equation (6) and evaluating it numerically for $\omega = \omega_\Lambda = 2\pi/\tau_\Lambda$. Assuming strong entanglement, $L \gg \Lambda$, and with the substitution $n \to z = n\ (\Lambda/L)$, the sum can be approximated by the following integrals:

$$\alpha_f(\omega) \approx \frac{\Lambda^4}{k_B T \pi^4 l_p^2} \left\{ \int_1^\infty dz \frac{1}{z^4 + z^2 f/f_\Lambda + i\,\omega\tau_\Lambda/2} + \int_0^1 dz \frac{1}{z^4 + z^2 f/f_\Lambda + i\,\omega\tau_\Lambda/2 \exp[\mathcal{E}(1/z - 1)]} \right\}. \tag{7}$$

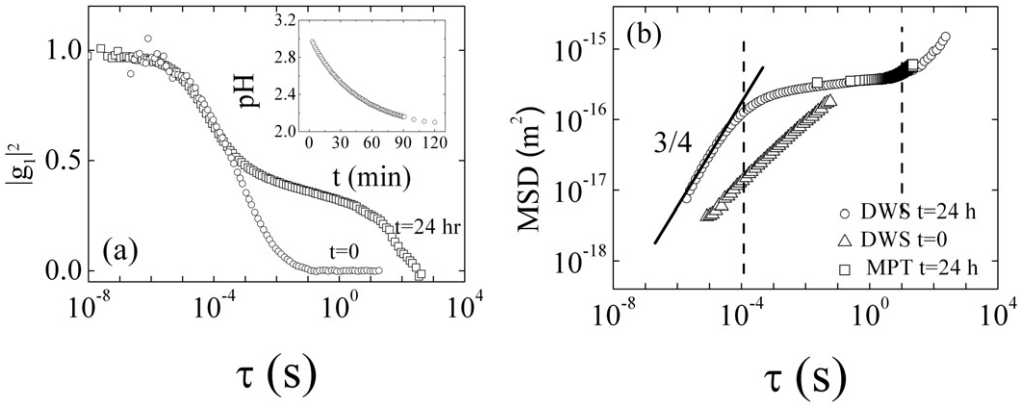

Figure 2. (a) De-correlation of scattered laser light induced by the movement of microspheres within a sample of the engineered DM42 blocky-pectin recorded immediately, and 24 h after, the introduction of GDL at 25 °C. The inset shows the rate of the pH decrease induced by the hydrolysis of the GDL. (b) The corresponding MSD of the probe particles.

The prestress σ is related to the tension f via

$$\sigma = \frac{f}{5\xi^2}. \tag{8}$$

2.5.2. Mean-square displacement. The transverse mean-square displacement (MSD) of the polymer backbone, which we assume to be proportional to the MSD of the embedded microspheres, is given by

$$\delta r_\perp^2(t) = \frac{4L^3}{l_\mathrm{p}\pi^4} \sum_n \frac{1-\exp(-t/\tilde{\tau}_n)}{n^4 + n^2 f/f_L}. \tag{9}$$

Analogous to the procedure for the susceptibility in the preceding section the sum can be approximated by the following integrals:

$$\delta r_\perp^2(t) \approx \frac{4\Lambda^3}{l_\mathrm{p}\pi^4} \left\{ \int_1^\infty \mathrm{d}z \frac{1-\exp[-t/\tau_\Lambda (z^4 + z^2 f/f_\Lambda)]}{z^4 + z^2 f/f_\Lambda} + \int_0^1 \mathrm{d}z \frac{1-\exp[-t/\tau_\Lambda (z^4 + z^2 f/f_\Lambda)\mathrm{e}^{-\mathcal{E}(1/z-1)}]}{z^4 + z^2 f/f_\Lambda} \right\}. \tag{10}$$

3. Results and discussion

3.1. Diffusing wave spectroscopy

Figure 2(a) shows the de-correlation of scattered laser light induced by the movement of microspheres within a 1% solution of the engineered DM42 blocky pectin, recorded both immediately and 24 h after the introduction of GDL at 25 °C. The inset shows the rate of the pH decrease induced by the hydrolysis of the GDL. In particular it is noteworthy that the pH was stable within uncertainties at around (2.1±0.1) when the measurements were taken in the

gelled state. There is a clear change in the form of the correlation function as the acidification induces interactions between the chains and a network is formed. While generally reminiscent of the behaviour of glasses and the qualitative form predicted by mode-coupling theory [51] the correlation function of the gel does ultimately show ergodic behaviour and figure 2(b) shows the derived MSD of the tracer particles corresponding to the recorded correlation function.

3.1.1. Short times: $\tau < 0.1\,ms$. The high-frequency (short-time) data reveals that the MSD of the tracer particles scales with lag time according to a power law with an exponent close to 0.75 of (0.76±0.01). This behaviour has also been seen in previous experiments carried out on calcium-induced pectin gels, where it was assumed to arise from the fact that the persistence length of the network strands was an appreciable fraction of the mesh size so that the bending of semi-flexible entities dominates the resistance to small displacements of the tracer particles. Indeed, many hierarchically assembled biopolymer networks have been found to behave as semi-flexible networks [2–10, 52, 53], as exemplified by F-actin. In previous work on calcium-induced pectin gels, the proposal that the 3/4 power law scaling found at short times was a strong signature of the bending undulations of individual semi-flexible polymers was supported by TEM and small angle x-ray scattering (SAXS) data [54], and carrying out such studies of the current acid gel systems forms part of ongoing work.

3.1.2. Intermediate times: $0.1\,ms < \tau < 10\,s$. While the short-time behaviour exhibited by the tracer particles embedded in the acid-gels studied herein echoes that observed in the previously studied calcium-induced networks, the longer time behaviour is strikingly different. Whereas a largely time-independent elastic plateau is observed for calcium-induced gels (as expected for long-lived cross-links), the acid-gels clearly show some time dependency in this regime (figure 2(b)). Such behaviour has been demonstrated for F-actin networks [17] and living cells [55] and is thought to arise from the thermally activated release of weak cross-links permitting the sliding of network chains. Its observation in our measurements could indicate that the binding energies of the putative hydrogen bonded cross-links are less than those associated with the ionic bonding in the previously studied systems, as might be expected. In order to pursue the molecular nature of the associations, the experiment was repeated in the presence of urea, a recognized hydrogen-bond breaker. Figure 3(a) shows these results along with fits to the GWLC model. It can be seen that (i) the GWLC model provides an excellent description of the microrheological data exhibited by these systems over some six orders of magnitude in time, (ii) that the insensitivity of the 3/4 scaling region to the presence of urea confirms its origin in the mechanics of single filament deformations and (iii) that the increased mobility of tracer particles upon increasing the urea concentration supports the hypothesis that hydrogen bonds are largely responsible for the formation of the cross-links.

The experiments were repeated for a number of polymer concentrations. Despite the fact that a plateau in the MSD data at the lower frequencies was not strictly observed, the value of the MSD in this slowly varying intermediate region (at 0.1 s) was recorded and is plotted in figure 3(b). It can be seen that the concentration dependence of this quasi-plateau value is close to a power law scaling with an exponent of 1.4; as was found in previous work on calcium mediated pectin networks and indeed as predicted for lightly cross-linked semi-flexible networks [7, 10]. Thus, the microrheological properties of acid pectin gels over the frequency range from $1–10^6$ Hz are well captured by a model of self-assembled semi-flexible filaments, with weak hydrogen-bonded connections permitting slippage at longer timescales.

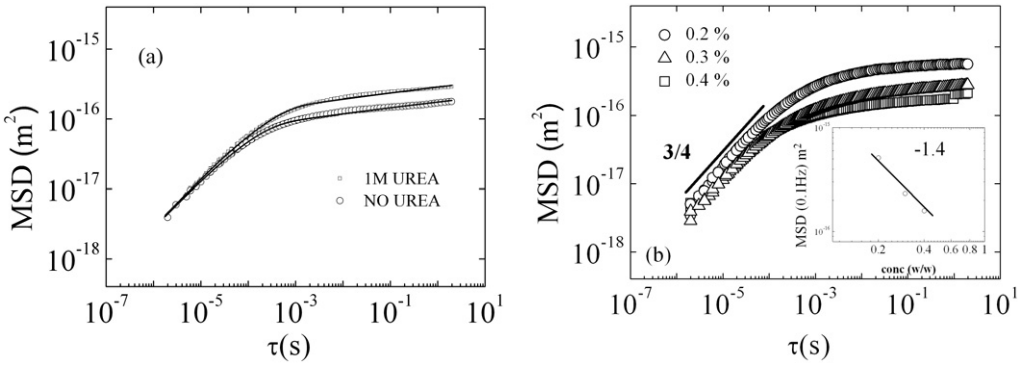

Figure 3. (a) MSD of tracer particles as obtained by DWS measurements: 0.4wt% DM42 acid induced gel, and the same gel formed in the presence of 1 M urea. (Only every third data-point is shown for clarity.) The lines are the best fits from the GWLC model, with $\Lambda = 0.1215\,\mu$m (lower curve), $0.146\,\mu$m (upper curve), $\zeta_\perp = 0.223$ Pa s, $\mathcal{E} = 26$ and $l_p = 0.3\,\mu$m as for the fits in the temperature dependent data discussed in due course. (b) The value of the MSD in the slowly varying intermediate region for a set of experiments performed at low concentrations (at 0.1 s). It can be seen that the concentration dependence of this quasi-plateau value is close to a power law with an exponent of 1.4 as expected for semiflexible polymer networks [3, 5, 38, 53, 65, 66].

3.1.3. Long times: $\tau > 10\,s$. Over longer timescales still another process is observed that completely de-correlates the scattered light and manifests as the MSD increasing as a power law with a sub-diffusive exponent that is substantially greater than that found at intermediate times. MPT experiments were subsequently undertaken in this regime in order to validate the observed phenomena and investigate the possibility that it arises from dynamical heterogeneities or the 'pore-hopping' behaviour of a sub-population of beads. While the latter process has previously been observed in F-actin networks when the size of the tracer particles approached that of the mesh [56], in this system a uniform mesh size is estimated to be an order of magnitude smaller than the probes.

3.2. Multiple-particle tracking

Figure 2(b) includes the ensemble-averaged MSD from the MPT experiments compared with that obtained from DWS. The MPT result has been scaled to three dimensions and additionally by a factor to account for slight differences in probe size between the two experiments. It can be seen that there is reasonable agreement between the results of the two independent experiments suggesting that indeed the long-time behaviour observed is physically meaningful. Figure 4(a) shows the ensemble-averaged MSD, while figures 4(b) and (c) show Van Hove plots of the probe particles displacements and a selection of individual particle trajectories, respectively, calculated for several time lags within the intermediate and long-time regimes. Van Hove plots calculated for times less than 1 s could all be very clearly described by Gaussian distributions, suggesting a unambiguously dynamically homogeneous system over these timescales. For sampling displacements over the scarcer longer time intervals the statistics become substantially worse, and while there are no clear indications in the Van Hove plots of sub-populations of probe

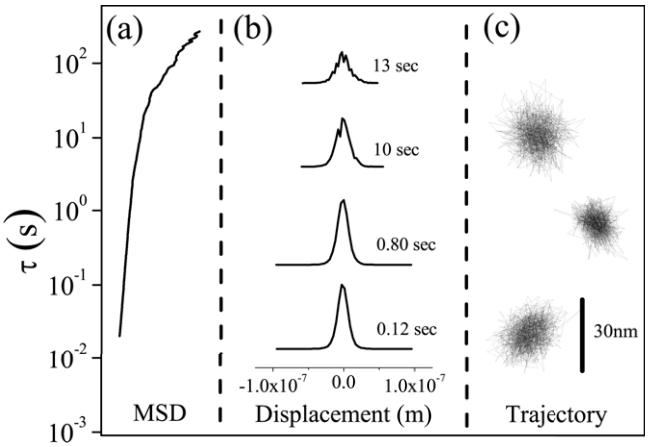

Figure 4. (a) The ensemble-averaged MSD obtained from the MPT experiments carried out on a gelled sample of the engineered DM42 blocky-pectin recorded 24 h after the introduction of GDL at 25 °C. Panels (b) and (c) show Van Hove plots of the probe particles displacements and a selection of individual particle trajectories respectively, calculated for a variety of times lags within the short, intermediate and long-time regimes.

particles moving in different micromechanical environments (figure 4) it is difficult to eliminate such a possibility completely. All individual trajectories appear similar by eye, as illustrated in the figure, with typical dimensions on the order of less than one tenth of the beads size.

3.3. Nonlinear rheology: stress-stiffening experiments

Nonlinear rheological measurements provide a further critical test to assess how far the similarity between our pectin gels and cytoskeletal and extra-cellular networks extends. They also allow for a more thorough investigation of the utility of the GWLC model in capturing the essential behaviour of the acid-induced pectin networks. Stress-stiffening experiments were performed on the microrheologically-interrogated systems as described in the experimental section. Figure 5 shows the scaled normalized differential shear modulus of pectin plotted against the scaled prestress, where three regimes can be distinguished. At low stress, it is approximately constant, meaning that the stress–strain relation is linear. Above a certain stress, one observes a stiffening with increasing prestress, until it drops sharply.

3.3.1. Temperature dependence of nonlinear rheology. Of particular interest to us is the dependence of the stress-stiffening response on temperature. The data in figure 5 reveal a characteristic reduction in the stiffening response of the differential shear modulus as the temperature increases by a few degrees. The measurements were performed at four different temperatures, 10, 20, 30 and 40 °C. Temperature enters the model via different pathways. The solvent viscosity decreases with temperature and is estimated using the empirical Vogel–Fulcher relation

$$\eta(T) = \eta_\infty \exp\left(\frac{A}{T - T_{\mathrm{VF}}}\right) \tag{11}$$

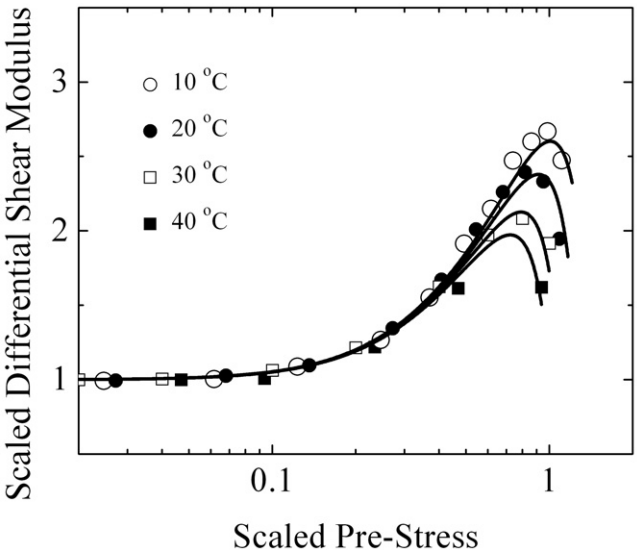

Figure 5. Differential modulus plotted against the pre-stress, scaled by the zero-pre-stress differential modulus, for a 1% w/w pectin solution (DM42) acidified to pH 2 by GDL, at four different temperatures. Fitted with the assumptions described in the text and the following parameters: $l_p = 0.3\,\mu$m, $\xi = 0.01\,\mu$m, $\mathcal{E} = 32$ for $T = 30\,^\circ$C, $\zeta_\perp = 62.17\eta$, $c = 0.439$. The effective barrier width Δ and the distance Λ between closed bonds as a function of temperature are plotted in figures 6(a) and (b).

with the parameters for H_2O, $\eta_\infty = 0.02984$ mPa s, $A = 496.9$ K and $T_{VF} = 152.0$ K. This affects the transverse friction coefficient which is proportional to η. In the nonlinear regime, the effect of the temperature dependence of the viscosity on the differential shear modulus is negligibly small, but it cannot be neglected for linear measurements, as we will see in the following section for the MSD. Besides the viscosity, the bending rigidity $\kappa = k_B T l_p$ and the dimensionless effective barrier height, $\mathcal{E}$, depend on temperature. The precise functional for the experimental system is unknown. While any relation of the form $\kappa, \mathcal{E}^{-1} \propto T^x$ with $0 \leqslant x \leqslant 1$ seems physically plausible, the precise value of the exponent x only affects the predictions of the model relatively mildly. In contrast the model predictions turn out to be more sensitive to the structural properties encoded in the crossover scale Λ and the bond length Δ, for which even a weak temperature dependence matters. For the fits in figure 5, a linear increase of Δ with temperature is assumed, as shown in figure 6(a).

Furthermore, there seems to be a small signature of the fact that the pectin sample was prepared at room temperature and then heated up or cooled down to the temperature of study, as seen from the slight but significant deviations of the best-fitting values for Λ from the average (figure 6(b)). While such temperature-history dependent effects can be seen to be minor in these thermoreversible gels, it is possible that trapping and annealing effects might be detectable. The slight increase of Λ for temperatures of 10 and 20 °C might be interpreted as an indication that the fraction of closed bonds is slightly reduced when the sample is cooled instead of heated. This is in accordance with the results of several stiffness measurements for pectin [31], but also for other polysaccharides, such as κ-carrageenan [57] or agarose [58]. In these experiments, it has been observed that the stiffness of the polysaccharide networks was higher when the sample is

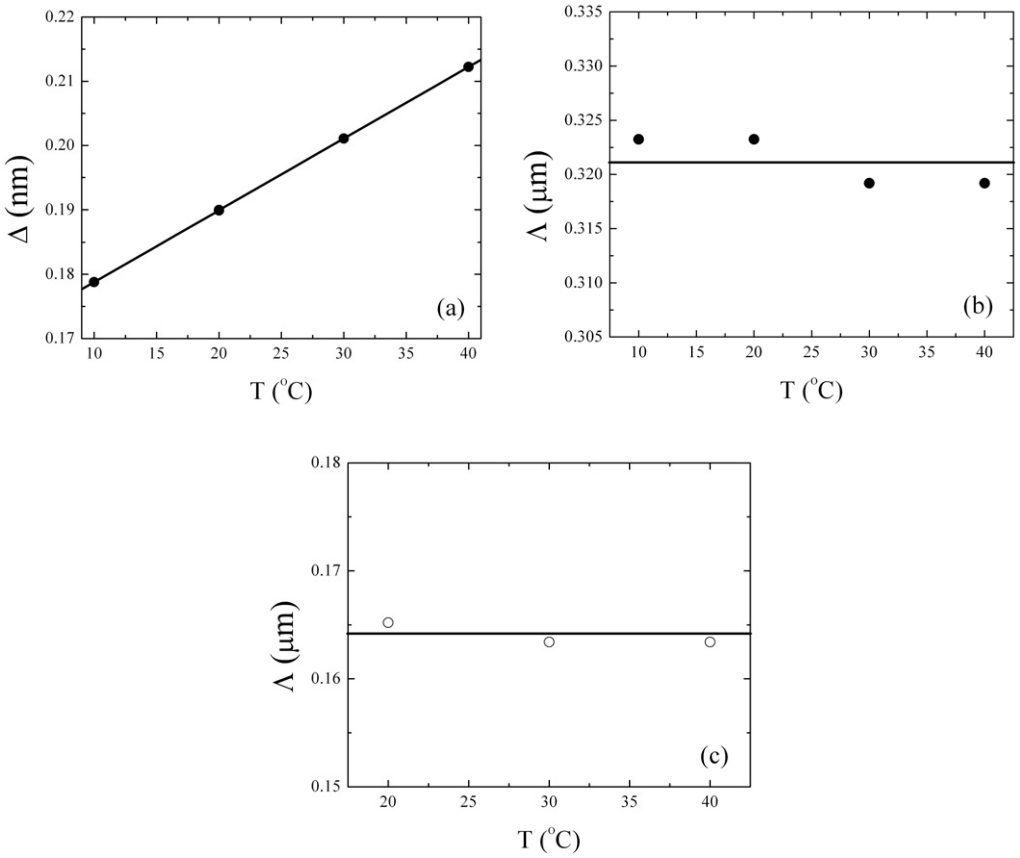

Figure 6. (a), (b) Effective barrier width Δ and distance Λ between closed bonds as a function of temperature used for the fits in figure 5. (c) Distance between closed bonds used for the fits in figure 7. That the relevant interaction scale appears slightly larger if deduced from nonlinear as opposed to linear rheology, is in line with numerical simulations of transiently crosslinked semiflexible polymer networks [63].

heated up to a certain temperature compared to the case when it is cooled down to it. Attributing a lower stiffness to a lower fraction of closed bonds, and thus a larger distance Λ between neighbouring bonds for the cooling process, our data seem consistent with these studies.

To produce the fits of the data shown in figure 5, we used the parameters $\mathcal{E}/k_{\mathrm{B}}T$=32 for $T = 30\,^{\circ}\mathrm{C}$, $c = 0.439$ and $\zeta_{\perp}(T) = 62.17\eta(T)$, where $\eta(T)$ is the viscosity of water. The effective bond length in the order of $\Delta = 0.2\,\mathrm{nm}$ is compatible with the length of a hydrogen bridge bond, and the persistence length of $l_{\mathrm{p}} = 0.3\,\mu\mathrm{m}$ is in agreement with previous results [10]. Since l_{p} is a measure for the stiffness, the dominant pectin mesostructures are softer than actin, the persistence length of which is about $l_{\mathrm{p}} = 10\,\mu\mathrm{m}$. The GWLC model suggests that the temperature dependence of the dynamics originates in the microscopic structure of the weakly adhesive interactions constituting the mesoscale network, which are summarily represented by the effective bond parameter $\Delta(T)$. Its temperature dependence could hint at a water-specific effect, which would however need to be biopolymer-specific, and in particular, be much more pronounced for actin than for pectin. The effective distance $\Lambda = 0.32\,\mu\mathrm{m}$ between

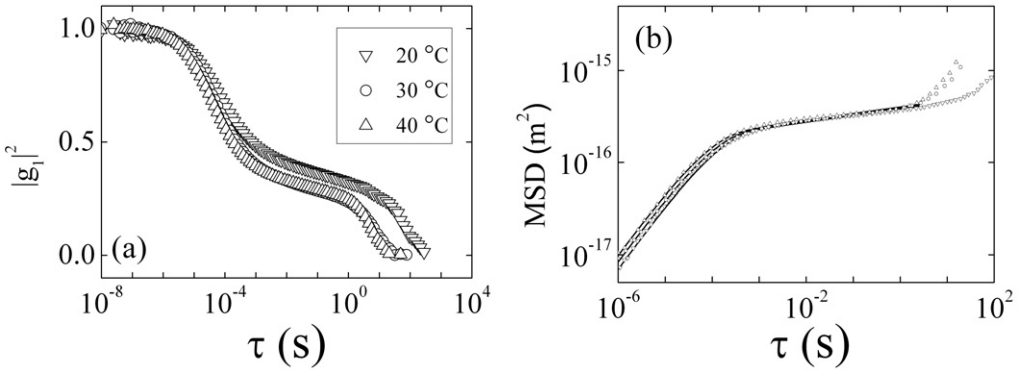

Figure 7. (a) De-correlation of scattered laser light induced by the movement microspheres within a sample of the engineered DM42 blocky-pectin recorded 24 h after the introduction of GDL. After the gel had formed experiments were carried out as a function of temperature between 20 and 40 °C. (b) The corresponding MSD of the probe particles for the data shown in (a). MSD as a function of time at different temperatures, 20, 30 and 40 °C (bottom to top), fitted with the GWLC using the same values for l_p, $\mathcal{E}$, $\zeta_\perp$ as for the nonlinear fits in the preceding section and Λ as plotted in figure 6(c).

closed bonds is larger than the mesh size $\xi = 0.01\ \mu$m estimated via equation (8) from the ratio of the experimentally applied stress to the backbone tension used for the fits. While generally consistent with the weakly sticky interaction suggested by the rest of the analysis, a clear-cut geometric interpretation of this observation seems elusive, given the schematic level of modelling (neglecting important elements of the geometry of bond loading) and the fact that the amount of polymer effectively contributing to the stress-bearing meso-structure is not known.

Indeed, these experiments show the clear stress-stiffening and eventual softening as is predicted by the same GWLC model that described the microrheological response so well [12, 17] and the sensitive dependence of its strength on various parameters such as temperature and polymer concentration that has previously been observed in many biopolymer networks (F-actin [12], intermediate filaments [59, 60], microtubule–actin mixtures [61] and collagen [62]).

3.4. Temperature dependence of microrheological experiments

Inspired by the ability of the GWLC to capture the temperature dependence of the nonlinear behaviour, the microrheological study was revisited and the DWS experiments were repeated as a function of temperature (figure 7). After the gel had formed experiments were carried out as a function of temperature between 20 and 40 °C. It was noted that any differences in the pH caused by the temperature changes were minimal (<0.2). Samples were left to equilibrate for 30 min at each temperature before the measurements were made. On revisiting previous temperatures minimal hysteresis was observed. Interestingly, while the behaviour on short and intermediate times did not significantly change over the relatively small temperature range that could be practically investigated at present, the terminal de-correlation of the scattered light described above, showed a clear evolution with temperature. On increasing the temperature such behaviour can be observed at shortened timescales and with an increasing terminal relaxation

rate (figure 7). Neglecting these terminal decay processes then it could be said that whereas in the nonlinear regime the stiffness of the pectin gels investigated decreases noticeably with increasing temperature, in the linear regime the effect of temperature is small.

The predictions of the GWLC model, given by the result of the numerical evaluation of equation (10) for vanishing prestress are shown by the black curves in figure 7. Except for the distance Λ between closed bonds, which is plotted in figure 6(c), the parameters are the same as used in the preceding section in order to successfully fit the nonlinear data. The different values of Λ may be related to the fact that different susceptibilities determine the behaviour. Whereas the nonlinear response is described by the longitudinal susceptibility, the linear response is described by the transversal susceptibility. As a comprehensive recent numerical investigation of an elaborate model for reversibly crosslinked semiflexible polymer networks emphasized, the linear rheology is governed by non-affine bending deformations and entanglements, but the nonlinear rheology by predominantly affine filament stretching between crosslinks [63]. Each type of measurement is demonstrated to have its own characteristic interaction length scale, consistent with our findings.

The slight increase of the MSD with temperature at short times is mainly due to the decreasing solvent viscosity according to the Vogel–Fulcher relation, equation (11); while at intermediate times, temperature enters mainly via the barrier height $\mathcal{E}$, and the data are consistent with the presumed standard Arrhenius behaviour $\mathcal{E} \propto T^{-1}$. We do not attempt here to model the terminal relaxation for $\tau > 10\,\mathrm{s}$, the investigation of which remains a focus for our continued investigations. It is clear that the otherwise relative insensitivity of the linear microrheological properties on temperature is well captured within the GWLC framework, despite the substantial temperature dependence of the nonlinear properties.

3.4.1. Comparison with experimental data from other systems. As for pectin, the stiffness of F-actin decreases with temperature [17]. To compare the actin data to the pectin data recorded for the acid-gels investigated here, the characteristic slope x of the scaled normalized differential shear modulus has been determined for the data shown in figure 5 and plotted alongside the normalized inverse of the creep compliance of F-actin measured in previous work (figure 8(a)). On average, a temperature increase of 10 °C causes a decrease of the slope by about 18% for this pectin system, compared to about 150% for F-actin. Additionally, we determined the scaled peak stiffness for the F-actin and the pectin data, shown in figure 8(b). For F-actin, a temperature increase of 10 °C decreases the peak value of the normalized inverse creep compliance by about 90%, while for pectin, a temperature increase of 10 °C causes a decrease of the scaled peak stiffness by about 13%.

A decrease of stiffness with temperature has also been observed in non-adherent THP-1 cells [64]. In this work the Young's modulus, which was determined from atomic force microscope (AFM) force measurements, decreased from 3.2 to 0.5 kPa within a temperature range of 21 °C, so that for a temperature change of 10 °C, the stiffness decreased by around 60%. In summary, it can be stated that an increase in temperature causes a decrease of the stiffness of acid–pectin gels, as well as of F-actin networks and non-adherent THP-1 cells, but that the temperature effect at least for our particular pectin systems, is less pronounced. The different extent to which temperature changes affect the nonlinear rheology in pectin, actin and cellular systems is of fundamental interest. It is, to date, unclear whether these differences arise on the microscopic scale or rather depend on the mesoscale network architecture. Interestingly the analysis in our paper shows that the temperature effects for pectin acid-gels are quantitatively

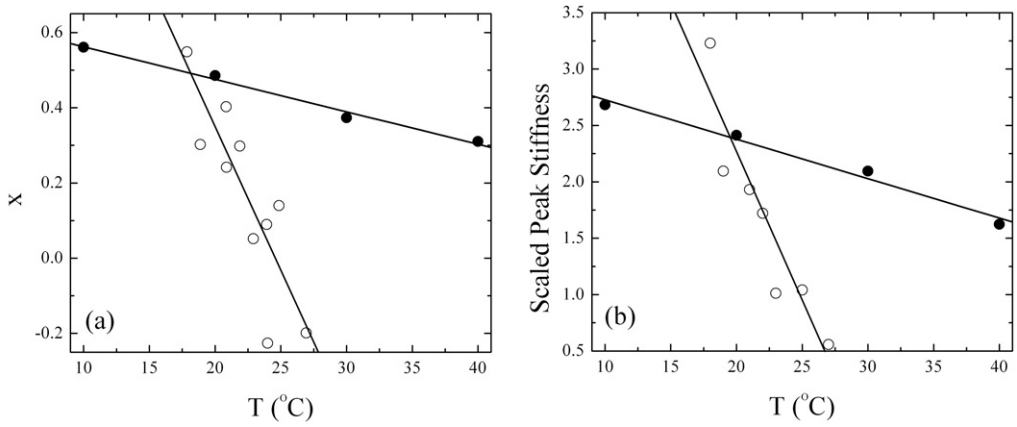

Figure 8. (a) Slope of the normalized inverse creep compliance and differential modulus, respectively, plotted against the temperature for actin (open circles) and pectin (filled circles). (b) Scaled peak stiffness plotted against the temperature for actin (open circles) and pectin (filled circles). The actin data are taken from [17].

parametrized by a generic polymer-based model (the GWLC), and could be indicative of a somewhat special mechanism at work in F-actin and cells.

4. Conclusion and outlook

The pursuit to understand the mechanics of the cytoskeleton has already driven forward great advances in experimental and theoretical areas of microrheology and semi-flexible network theories. Herein we have studied a polysaccharide network, whose understanding promises to enlighten another considerably less-studied, but arguably just as important, biopolymer matrix, that of the plant cell wall. It has been shown that the study of these systems too can benefit hugely from what has already been achieved in the understanding of reconstituted protein matrices and the application of mesoscopic models of semi-flexible filaments and glassy dynamics. We have revealed striking analogies between the rheological behaviour of acid pectin gels with molecularly highly dissimilar polymeric systems such as F-actin, intermediate filament and collagen networks. We rationalized the discovered similarity and the corresponding redundancy with respect to the molecular structure within a schematic mesoscopic polymer model that provides a faithful and consistent parametrization of our linear and nonlinear rheological data, obtained by various measurement techniques. Furthermore, at least for pectin and F-actin, the nonlinear response is found to be much more sensitive to temperature changes than their linear response, a property that is well reproduced by the GWLC model.

As an outlook, this work suggests that polysaccharide networks such as the pectin gels studied here are also promising model systems in their own right for testing and developing mesoscopic theories such as the GWLC model, with their own set of control parameters. In particular, the ability to modify the molecular architecture of the extended cross-linking sites (via the manipulation of the methylester pattern) holds the tantalizing possibility of controlling the junction zone ‘stickiness’ in a systematic way. Additionally using different assembly modalities offers the potential of modifying the mesoscopic network architecture in a controlled way while studying the resulting effects on the temperature sensitivity of the nonlinear rheology.

In general, mesoscopic physical models offer the potential to understand how, in principle, mechanical functionality at the cellular level arises from microscopic interactions. They aim to elucidate how a myriad of available molecular level control parameters, ranging from enzymatic modification of polymeric structure to local manipulation of pH and ionic strength, act within a unified framework to achieve the manipulation of the free-energy landscape governing the strength and dynamics of stress-bearing associations. In this way the apparent complexity of the biological can be seen as ensuring the provision of multiple pathways for controlling the same essential physics, with the redundancy not only introducing robustness in the system, but providing mechanisms for compensation, adaptation and homeostasis.

Acknowledgments

We thank Christian Secker for help in the early acid-gel work and Jens Glaser for initial work on the application of the GWLC. RRRV acknowledges AMI (Fribourg) for the use of the ARG2 rheometer. Allan Raudsepp and Yacine Hemar are gratefully acknowledged for interesting discussions.

References

[1] Bausch A R and Kroy K 2006 A bottom-up approach to cell mechanics *Nature Phys.* **2** 231–4
[2] Storm C, Pastore J J, MacKintosh F C, Lubensky T C and Janmey P A 2005 Nonlinear elasticity in biological gels *Nature* **435** 191–4
[3] Apgar J, Tseng Y, Fedorov E, Herwig M B, Almo S C and Wirtz D 2000 Multiple-particle tracking measurements of heterogeneities in solutions of actin filaments and actin bundles *Biophys. J.* **79** 1095–106
[4] Gardel M L, Shin J H, MacKintosh F C, Mahadevan L, Matsudaira P and Weitz D A 2004 Elastic behavior of cross-linked and bundled actin networks *Science* **304** 1301–5
[5] Palmer A, Xu J Y, Kuo S C and Wirtz D 1999 Diffusing wave spectroscopy microrheology of actin filament networks 1999 *Biophys. J.* **76** 1063–71
[6] Mason T G, Gisler T, Kroy K, Frey E and Weitz D A 2000 Rheology of F-actin solutions determined from thermally driven tracer motion *J. Rheol.* **44** 917–28
[7] Mackintosh F C, Kas J and Janmey P A 1995 Elasticity of semi-flexible biopolymer networks *Phys. Rev. Lett.* **75** 4425–8
[8] Mason T G, Dhople A and Wirtz D 1997 *Statistical Mechanics in Physics and Biology* ed D Wirtz and T C Halsey (Pittsburgh, PA: MRS) pp 153–8
[9] Willenbacher N, Oelschlaeger C, Schopferer M, Fischer P, Cardinaux F and Scheffold F 2007 Broad bandwidth optical and mechanical rheometry of wormlike micelle solutions *Phys. Rev. Lett.* **99** 068302
[10] Vincent R R, Pinder D N, Hemar Y and Williams M A K 2007 Microrheological studies reveal semiflexible networks in gels of a ubiquitous cell wall polysaccharide *Phys. Rev.* E **76** 031909
[11] Doi M and Edwards S F 1988 *The Theory of Polymer Dynamics* (Oxford: Clarendon)
[12] Kroy K and Glaser J 2007 The glassy wormlike chain *New J. Phys.* **9** 416–27
[13] Sollich P, Lequeux F, Hebraud P and Cates M E 1997 Rheology of soft glassy materials *Phys. Rev. Lett.* **78** 2020–3
[14] Sollich P and Cates M E 2012 Thermodynamic interpretation of soft glassy rheology models *Phys. Rev.* E **85** 031127
[15] Glaser J, Hallatschek O and Kroy K 2008 Dynamic structure factor of a stiff polymer in a glassy solution *Eur. Phys. J.* E **26** 123–36
[16] Kroy K 2008 Dynamics of wormlike and glassy wormlike chains *Soft Matter* **4** 2323–30

[17] Semmrich C, Storz T, Glaser J, Merkel R, Bausch A R and Kroy K 2007 Glass transition and rheological redundancy in F-actin solutions *Proc. Natl Acad. Sci. USA* **104** 20199–203
[18] Wolff L, Fernandez P and Kroy K 2010 Inelastic mechanics of sticky biopolymer networks *New J. Phys.* **12** 053024
[19] Willats W G T, Knox P and Mikkelsen J D 2006 Pectin: new insights into an old polymer are starting to gel *Trends Food Sci. Technol.* **17** 97–104
[20] Peaucelle A, Braybrook S and Hofte H 2012 Cell wall mechanics and growth control in plants: the role of pectins revisited *Front. Plant Sci.* **3** 121
[21] Vincken J P, Schols H A, Oomen R, McCann M C, Ulvskov P, Voragen A G J and Visser R G F 2003 If homogalacturonan were a side chain of rhamnogalacturonan: I. Implications for cell wall architecture *Plant Physiol.* **132** 1781–9
[22] Gidley M J, Morris E R, Murray E J, Powell D A and Rees D A 1980 Evidence for 2 mechanisms of interchain association in calcium pectate gels *Int. J. Biol. Macromol.* **2** 332–4
[23] Morris E R, Gidley M J, Murray E J, Powell D A and Rees D A 1980 Characterization of pectin gelation under conditions of low water activity by circular dichroism, competitive inhibition and mechanical properties *Int. J. Biol. Macromol.* **2** 327–30
[24] Morris E R, Powell D A, Gidley M J and Rees D A 1982 Conformations and interactions of pectins: 1. Polymorphism between gel and solid states of calcium polygalacturonate *J. Mol. Biol.* **155** 507–16
[25] Powell D A, Morris E R, Gidley M J and Rees D A 1982 Conformations and interactions of pectins: 2. Influence of residue sequence on chain association in calcium pectate gels *J. Mol. Biol.* **155** 517–31
[26] Parre E and Geitmann A 2005 Pectin and the role of the physical properties of the cell wall in pollen tube growth of Solanum chacoense *Planta* **220** 582–92
[27] Vincent R, Cucheval A, Hemar Y and Williams M 2009 Bio-inspired network optimization in soft materials—insights from the plant cell wall *Eur. Phys. J.* E **28** 79–87
[28] Vincent R R and Williams M A K 2009 Microrheological investigations give insights into the microstructure and functionality of pectin gels *Carbohydrate Res.* **344** 1863–71
[29] O'Brien A B, Philp K and Morris E R 2009 Gelation of high-methoxy pectin by enzymic de-esterification in the presence of calcium ions: a preliminary evaluation *Carbohydrate Res.* **344** 1818–23
[30] Slavov A, Garnier C, Crepeau M J, Durand S, Thibault J F and Bonnin E 2009 Gelation of high methoxy pectin in the presence of pectin methylesterases and calcium *Carbohydrate Polym.* **77** 876–84
[31] Gilsenan P M, Richardson R K and Morris E R 2000 Thermally reversible acid-induced gelation of low-methoxy pectin *Carbohydrate Polym.* **41** 339–49
[32] Strom A, Ribelles P, Lundin L, Norton I, Morris E R and Williams M A K 2007 Influence of pectin fine structure on the mechanical properties of calcium–pectin and acid–pectin gels *Biomacromolecules* **8** 2668–74
[33] Ravanat G and Rinaudo M 1980 Investigation on oligogalacturonic and polygalacturonic acids by potentiometry and circular-dichroism *Biopolymers* **19** 2209–22
[34] Cesaro A, Ciana A, Delben F, Manzini G and Paoletti S 1982 Physiochemical properties of pectic acid: 1. Thermodynamic evidence of a pH-induced conformational transistion in aqueos solution *Biopolymers* **21** 431–49
[35] Jarvis M C and Apperley D C 1995 Chain conformation in concentrated pectic gels—evidence form C-13 NMR *Carbohydrate Res.* **275** 131–45
[36] Walkinshaw M D and Arnott S 1981 Conformations and interactions of pectins: 1. X-ray diffraction of sodium pectate in neutral and acidified forms *J. Mol. Biol.* **153** 1055–73
[37] Walkinshaw M D and Arnott S 1981 Conformations and interactions of pectins: 2. Models for junction zones in pectinic acid and calcium pectate gels *J. Mol. Biol.* **153** 1075–85
[38] Gittes F and MacKintosh F C 1998 Dynamic shear modulus of a semiflexible polymer network *Phys. Rev.* E **58** 1241–44
[39] Williams M A K, Foster T J and Schols H A 2003 Elucidation of pectin methylester distributions by capillary electrophoresis *J. Agric. Food Chem.* **51** 1777–81

[40] Williams M A K, Cucheval A, Ström A and Ralet M C 2009 Electrophoretic behavior of copolymeric galacturonans including comments on the information content of the intermolecular charge distribution *Biomacromolecules* **10** 1523–31
[41] Goubet F, Ström A, Dupree P and Williams M A K 2005 An investigation of pectin methylesterification patterns by two independent methods: capillary electrophoresis and polysaccharide analysis using carbohydrate gel electrophoresis *Carbohydrate Res.* **340** 1193–9
[42] Ström A and Williams M A K 2004 On the separation, detection and quantification of pectin derived oligosaccharides by capillary electrophoresis *Carbohydrate Res.* **339** 1711–6
[43] Hunt J J, Cameron R and Williams M A K 2006 On the simulation of enzymatic digest patterns: the fragmentation of oligomeric and polymeric galacturonides by endo-polygalacturonase II *Biochim. Biophys. Acta* **1760** 1696–703
[44] Edwards P J B, Kakubayashi M, Dykstra R, Pascal S M and Williams M A K 2010 Rheo-NMR studies of an enzymatic reaction: evidence of a shear-stable macromolecular system *Biophys. J.* **98** 1986–94
[45] Waigh T A 2005 Microrheology of complex fluids *Rep. Prog. Phys.* **68** 685–742
[46] Gittes F, Schnurr B, Olmsted P D, MacKintosh F C and Schmidt C F 1997 Microscopic viscoelasticity: shear moduli of soft materials determined from thermal fluctuations *Phys. Rev. Lett.* **79** 3286–9
[47] Mason T G, Ganesan K, van Zanten J H, Wirtz D and Kuo S C 1997 Particle tracking microrheology of complex fluids *Phys. Rev. Lett.* **79** 3282–5
[48] Hemar Y and Pinder D N 2006 DWS microrheology of a linear polysaccharide *Biomacromolecules* **7** 674–6
[49] Weitz D A and Pine D J 1993 *Dynamic Light Scattering: The Method and Some Applications* ed W Brown (Oxford: Oxford University Press) pp 652–720
[50] Fernandez P, Pullarkat P A and Ott A 2006 A master relation defines the nonlinear viscoelasticity of single fibroblasts *Biophys. J.* **90** 3796–805
[51] Götze W 2012 *Complex Dynamics of Glass–Forming Liquids: A Mode-Coupling Theory* (*International Series of Monographs on Physics*) (New York, NY: Oxford University Press)
[52] Koenderink G H, Atakhorrami M, MacKintosh F C and Schmidt C F 2006 High-frequency stress relaxation in semiflexible polymer solutions and networks *Phys. Rev. Lett.* **96** 138307
[53] Morse D C 1998 Viscoelasticity of tightly entangled solutions of semiflexible polymers *Phys. Rev.* E **58** R1237–40
[54] Schuster E, Cucheval A, Lundin L and Williams M A K 2011 Using SAXS to reveal the degree of bundling in the polysaccharide junction zones of microrheologically distinct pectin gels *Biomacromolecules* **12** 2583–90
[55] Kollmannsberger P and Fabry B 2011 *Annual Review of Materials Research* vol 41 ed D R Clarke and P Fratzl (Palo Alto, CA: Annual Reviews) pp 75–97
[56] Wong I Y, Gardel M L, Reichman D R, Weeks E R, Valentine M T, Bausch A R and Weitz D A 2004 Anomalous diffusion probes microstructure dynamics of entangled F-actin networks *Phys. Rev. Lett.* **92** 178101
[57] Piculell L, Borgström J, Chronakis I S, Quist P-O and Viebke C 1997 Organisation and association of κ-carrageenan helices under different salt conditions *Int. J. Biol. Macromol.* **21** 141–53
[58] Mohammed Z H, Hember M W N, Richardson R K and Morris E R 1998 Kinetic and equilibrium processes in the formation and melting of agarose gels *Carbohydrate Polym.* **36** 15–26
[59] Schopferer M, Bar H, Hochstein B, Sharma S, Mucke N, Herrmann H and Willenbacher N 2009 Desmin and vimentin intermediate filament networks: their viscoelastic properties investigated by mechanical rheometry *J. Mol. Biol.* **388** 133–43
[60] Lin Y C, Yao N Y, Broedersz C P, Herrmann H, MacKintosh F C and Weitz D A 2010 Origins of elasticity in intermediate filament networks *Phys. Rev. Lett.* **104** 058101
[61] Lin Y C, Koenderink G H, MacKintosh F C and Weitz D A 2011 Control of nonlinear elasticity in F-actin networks with microtubules *Soft Matter* **7** 902–6
[62] Kurniawan N A, Wong L H and Rajagopalan R 2012 Early stiffening and softening of collagen: interplay of deformation mechanisms in biopolymer networks *Biomacromolecules* **13** 691–8

[63] Kurniawan N A, Enemark S and Rajagopalan R 2012 The role of structure in the nonlinear mechanics of cross-linked semiflexible polymer networks *J. Chem. Phys.* **136** 065101

[64] Rico F, Chu C, Abdulreda M H, Qin Y and Moy V T 2010 Temperature modulation of integrin-mediated cell adhesion *Biophys. J.* **99** 1387–96

[65] Isambert H and Maggs A C 1996 Dynamics and rheology of actin solutions *Macromolecules* **29** 1036–40

[66] Hinner B, Tempel M, Sackmann E, Kroy K and Frey E 1998 Entanglement, elasticity and viscous relaxation of actin solutions *Phys. Rev. Lett.* **81** 2614–17